

Triphasic Nanocolloids

Kyung-Ho Roh, David C. Martin, and Joerg Lahann*

Macromolecular Science and Engineering Program, Department of Materials Science and Engineering, and Department of Chemical Engineering, University of Michigan, Ann Arbor, Michigan 48109

Received March 1, 2006; E-mail: lahann@umich.edu

One of the major challenges in current nanotechnology is the control of materials distribution at ultra-small length scales, potentially leading to the fabrication of multicompartmental nanoparticles. One of the simplest versions thereof are two-sided particles, so-called Janus particles, which are believed to be of importance for designing active nanostructures or as functional elements in future device generations.¹ As a first step toward the fabrication of multiphase nanocolloids, we recently reported on the use of electrified co-jetting as an alternative approach toward Janus-type nanocolloids.² The electrified co-jetting process exploits the manipulation of liquid jets with nanometer scale diameters created under the influence of electrohydrodynamic forces.³ The basic electrohydrodynamic process⁴ was applied to a broad range of materials, including polymer solutions,⁵ melts,⁶ blends,⁷ and dispersions.⁸

In this communication, we extended the concept of electrified co-jetting to the simultaneous manipulation of three distinct liquid flows, thereby establishing a versatile and simple avenue toward triphasic nanocolloids, that is, nanocolloids with three distinct compartments.

In our co-jetting experiments, a laminar flow of three distinct polymer solutions was pumped at suitable flow rates, typically in the range of microliters per minute, through a modified nozzle with side-by-side geometry.⁹ The schematic diagram of Figure 1a shows three parallel jetting capillaries used in a conventional electrified jetting setup. The capillaries are aligned to form a triangular cross-sectional geometry. Because the laminar flow regime extends through the needles into the outlet region, droplets with three distinct interfaces can be formed. Figure 1b shows an image of the outlet region during the jetting process, which consists of three fluid flows. The green, red, and blue jetting solutions are composed of poly(ethylene oxide) (PEO, MW 600 kD) mixed with different dyes: fluorescein-conjugated dextran (green), rhodamine B-conjugated dextran (red), and Alexa Fluor 647-conjugated bovine serum albumin (blue). From the digital image (Figure 1b) and the enlargement shown in Figure 1c, it is apparent that the three phases are maintained throughout the pendant droplet. Moreover, the digital image reveals a single liquid thread maintaining the interface between the three phases. The electrified co-jetting conditions were selected to ensure that the liquid jets ejected from the Taylor cone were fragmented to particles rather than extended to nanofibers (Supporting Information, Table S1).² Nevertheless, the co-jetting approach should be similarly extendable to the fabrication of tricompartmental nanofibers. Once the triphasic nanocolloids were prepared, we used confocal laser scanning microscopy (CLSM) and scanning electron microscopy (SEM) for characterization (Figure 2a and 2b). In the CLSM experiments, each fluorescent dye was excited with different lasers, and the individual compartments were observed in separate spectral windows. As shown in the overlay of the three confocal images (Figure 2a), the biomacromolecular dyes loaded into each jetting liquid remained compartmentalized

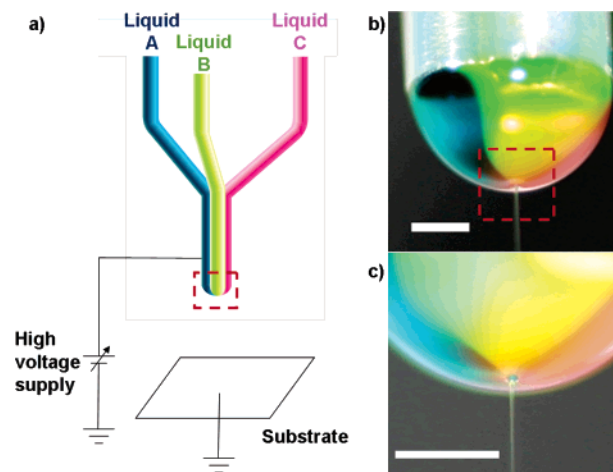


Figure 1. (a) Typical electrified jetting setup with triple side-by-side capillaries. (b) Actual photograph of the capillary outlet region designated with dotted line in (a). (c) Enlarged photograph of the jet ejection point designated with dotted line in (b). Scale bars are 500 μm .

to form separate phases. Figure 2a is a typical example of a CLSM snapshot of PEO-based triphasic particles. Although analysis of the triphasic geometry is occasionally challenging, our examination of multiple phase images confirms that almost every particle has three separate phases and is in agreement with data obtained for other polymers (Figure 2c–f, Supporting Information).

Figure 2b shows a SEM picture of PEG-based nanocolloids, which were still linked by fine polymer threads with diameters of the order of 10 nm (beads-on-a-string morphology). On the basis of the SEM analysis, the average diameter of the beads was determined to be 730 nm with a standard deviation of 260 nm.

In principle, jetting of polymer solutions under the influence of electrohydrodynamic forces can be applied to a wide range of commodity polymers. In addition to the PEO-based system, electrified co-jetting of either poly(acrylic acid) (PAA) or poly(acrylamide-co-acrylic acid) (PAAm-co-AA) solutions produced nanocolloids that resembled the PEO-based nanocolloids shown in Figure 2a.

The use of aqueous solutions for electrified co-jetting leads to nanocolloids that are inevitably water-soluble. Studying triphasic nanocolloids in aqueous environments will therefore require an extra modification step to stabilize the nanocolloids. The stabilization of polymer-based micro/nanostructures has been achieved by photochemical¹⁰ or thermal cross-linking.¹¹ To stabilize the triphasic nanocolloids, we turned to the thermal imidization, that is, the temperature-induced cross-linking of carboxylic acid groups of PAA with amide groups of PAAm.¹² We recently showed that thermal imidization can stabilize PAA- and PAAm-based nanocolloids.¹³

To probe the aqueous stability of tricompartmental particles cross-linked by thermal imidization, we incorporated differently colored biomacromolecular dyes into the aqueous solutions of poly-

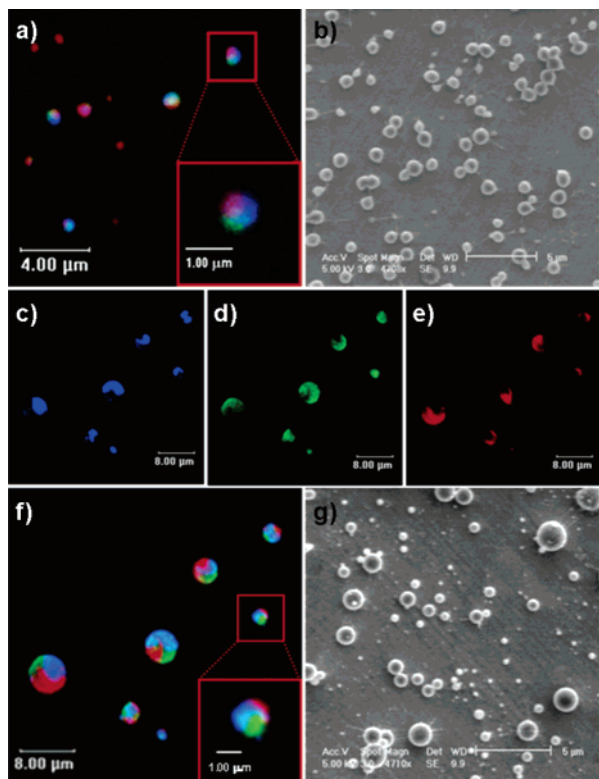


Figure 2. Confocal laser scanning microscopy image (a) and scanning electron microscopy of PEO particles (b). Confocal laser scanning microscopy images (c–f) and scanning electron microscopy (g) of colloidal particles made of P(AAm-co-AA) and PAA; the individual phases containing biomolecules labeled with FITC (c), rhodamine B (d), and Alexa Fluor 647 (e) and their overlay (f). CLSM image of (a) was obtained on top of a glass slide right after the jetting, while (c–f) were imaged from a suspension of the particles in water that had been thermally cross-linked after the jetting. Scale bars: 1 μm (inlets in a and f), 4 μm (a), 5 μm (b and g), 8 μm (c–f).

(acrylamide-co-acrylic acid, sodium salt) (MW 200 kD, 10% acrylic acid residues) and poly(acrylic acid) (MW 250 kD). After co-jetting and subsequent thermal cross-linking at 175 $^{\circ}\text{C}$ for 3 h, the nanocolloids were suspended in water and imaged by CLSM. In Figure 2c–e, individual compartments can be distinguished based on their characteristic fluorescent emission wavelength range, confirming that the biomolecules are localized in only a portion of each nanocolloidal particle even after the thermal treatment and suspension in water. The overlay of the three images (Figure 2f) clearly reveals predominant presence of each macromolecular dye in only one single phase. Occasionally, interfacial areas were observed, where two or more colors appeared to coexist. These limited findings suggest that some interfacial diffusion occurred during electrohydrodynamic processing and/or solidification. Once the nanocolloids are formed, intercompartmental diffusion of the macromolecular dyes is effectively prohibited by the formation of interpenetrating network between the cross-linked polymer matrixes and the biomacromolecular dyes. The integrity of the particles and the separate compartments of the dyes were maintained intact without dissolution or diffusion for an observed period of a few days (refer to Supporting Information, Figure S2, for details).

SEM analysis was performed on the tricompartmental PAA- and PAAm-based nanocolloids to complement the CLSM experiments. The SEM image shown in Figure 2g suggests that PAA- and PAAm-based nanocolloids are disconnected objects with close to perfectly spherical shapes. The mean diameter is about 430 nm with standard deviation of 400 nm. It should be noted that all size distributions were reported as observed, and no optimization with respect to controlling the size distributions was undertaken (refer to Supporting Information, Figures S3 and S4, for details). To obtain narrower size distributions and to approach the goal of a close to monodisperse size control, the combination of microfluidics-based hydrodynamic focusing¹⁴ and the use of polymers with a narrower molecular weight distribution should be pursued in further studies.

In summary, we have shown that macroscale fluid manipulation can be utilized for the fabrication of anisotropic nanoparticles with multiple compartmentalization. The fact that these novel nanocolloids are fabricated by electrified co-jetting suggests that the proposed technology may be broadly applicable to a wide range of different polymers and polymer composites in the fields of drug delivery, molecular imaging, and smart displays.

Acknowledgment. We thank Prof. Solomon, University of Michigan, for use of the confocal laser scanning microscope. D.C.M. acknowledges partial support from the National Science Foundation through Grant DMR-0084304.

Supporting Information Available: Detailed experimental procedures, additional confocal laser scanning microscopy data, and size distributions of the colloid particles. This material is available free of charge via the Internet at <http://pubs.acs.org>.

References

- (1) Perro, A.; Reculosa, S.; Ravaine, S.; Bourgeat-Lami, E.; Duguet, E. *J. Mater. Chem.* **2005**, *15*, 3745–3760.
- (2) Roh, K.-H.; Martin, D. C.; Lahann, J. *Nat. Mater.* **2005**, *4*, 759–763.
- (3) Zeleny, J. *Proc. Cambridge Philos. Soc.* **1915**, *18*, 71–83.
- (4) (a) Fong, H.; Chun, I.; Reneker, D. H. *Polymer* **1999**, *40*, 4585–4592. (b) Loscertales, I. G.; Barrero, A.; Guerrero, I.; Cortijo, R.; Marquez, M.; Gañán-Calvo, A. M. *Science* **2002**, *295*, 1695–1698. (c) Sun, Z.; Zussman, E.; Yarin, A. L.; Wendorff, J. H.; Greiner, A. *Adv. Mater.* **2003**, *15*, 1929–1932. (d) Li, D.; Xia, Y. N. *Nano Lett.* **2004**, *4*, 933–938.
- (5) Reneker, D. H.; Chun, I. *Nanotechnology* **1996**, *7*, 216–223.
- (6) Larrondo, L.; Manley R. S. J. *J. Polym. Sci., Part B: Polym. Phys.* **1981**, *19*, 909–920.
- (7) (a) Jin, H. J.; Fridrikh, S. V.; Rutledge, G. C.; Kaplan, D. L. *Biomacromolecules* **2002**, *3*, 1233–1239. (b) Kahol, P. K.; Pinto, N. J. *Synth. Met.* **2004**, *140*, 269–272. (c) Norris, I. D.; Shaker, M. M.; Ko, F. K.; Macdiarmid, A. G. *Synth. Met.* **2000**, *114*, 109–114.
- (8) (a) Yang, Q. B.; Li, D. M.; Hong, Y. L.; Li, Z. Y.; Wang, C.; Qiu, S. L.; Wei, Y. *Synth. Met.* **2003**, *137*, 973–974. (b) Sanders, E. H.; Kloefforn, R.; Bowlin, G. L.; Simpson, D. G.; Wnek, G. E. *Macromolecules* **2003**, *36*, 3803–3805.
- (9) (a) Gupta, P.; Wilkes, G. L. *Polymer* **2003**, *44*, 6353–6359. (b) Madhugiri, S.; Dalton, A.; Gutierrez, J.; Ferraris, J. P.; Balkus, K. J. *J. Am. Chem. Soc.* **2003**, *125*, 14531–14538.
- (10) Roffey, C. G. *Photogeneration of Reactive Species for UV-Curing*; Wiley: New York, 1997.
- (11) (a) Chapman, J. M.; Wyrick, S. D.; Voorstad, P. J. *J. Pharm. Sci.* **1984**, *73*, 1482–1484. (b) Maguire, J. H.; Dudley, K. H. *Anal. Chem.* **1977**, *49*, 292–297.
- (12) Yang, S. Y.; Rubner, M. F. *J. Am. Chem. Soc.* **2002**, *124*, 2100–2101.
- (13) Roh, K.-H.; Lahann, J. Manuscript in preparation.
- (14) (a) Utada, A. S.; Lorenceau, E.; Link, D. R.; Kaplan, P. D.; Stone, H. A.; Weitz, D. A. *Science* **2005**, *308*, 537–541. (b) Xu, S.; Nie, Z.; Seo, M.; Lewis, P.; Kumacheva, E.; Stone, H. A.; Garstecki, P.; Weibel, D. B.; Gitlin, I.; Whitesides, G. M. *Angew. Chem., Int. Ed.* **2005**, *44*, 724–728. (c) Sugiura, S.; Nakajima, M.; Itou, H.; Seki, M. *Macromol. Rapid Commun.* **2001**, *22*, 773–778. (d) Nisisako, T.; Torii, T.; Higuchi, T. *Chem. Eng. J.* **2004**, *101*, 23–29.

JA060836N